SUPPLEMENTARY MATERIAL

Interferometric detection of hydrodynamic bubble-bubble interactions

D. Raciti[1]†, P. Brocca[2], A. Raudino[3] and M. Corti[4]

[1]CNR-IMM, Zona Industriale VIII Strada 5, 95121 Catania, Italy.

[2]Department of Biotechnologies and Translational Medicine, University of Milan, LITA, via Fratelli Cervi 6 93, 20090 Segrate, Italy.

[3]Department of Chemical Sciences, University of Catania, Viale A. Doria 6, 95125 Catania, Italy.

[4]CNR-IPCF, Viale Ferdinando Stagno d'Alcontres 37, 98158 Messina, Italy.

Experimental details and control experiments

1. Sphericity of bubble oscillations

When the laser beam is focused on the bubble diameter, the fringe pattern observed in the backward direction is made of concentric circles (see Figure 1S). A static (non-spherical) deformation of the bubble would deform the fringe pattern. Deformation of the fringe pattern has never been observed along the experiments, thus ensuring valid operation of the interferometer. Measured amplitudes are of the order of 10 nm, that is 10^{-5} times the bubble diameter, with therefore negligible deformation of the bubble front and back curvatures and absolutely negligible influence on the interferometer operation.

The focusing point of the two interferometers of the experimental set-up (Figure 2S) can be easily moved sideways by micrometric screws (and piezo transducers for fine regulations), either for following independently bubble oscillations along their approach (goal of our experiment) or for checks of their performance. Directing the two interferometers onto the same bubble we obtained exactly the same resonance frequency and amplitude regardless of their different incidence angle.

2. Dependence of resonances on bubbles position

Experimental checks on the apparatus showed a slight variation (approximately 1%) of the measured resonant frequency when the position of the bubble in the cell was changed by 1 mm in the vertical direction (Oguz & Prosperetti 1990). Therefore, care was taken to perform measurements always at the same height from the cell bottom.

The uniformity of the pressure field in the cell provided by the piezo transducer was tested by means of the interferometer itself. A single bubble was scanned trough a horizontal line above the piezo. The resonance frequency remained practically unchanged (0,3% variation over a 2.5-mm scan), while the oscillation amplitude showed a smooth dependence (see Figure 3S), which was used to normalize amplitude data in the two-bubble experiments. The amplitude linearity of the piezo (Thorlab TA0505D024W) pressure transducer was experimentally checked by monitoring the oscillation amplitude of a single bubble. Doubling the applied voltage, oscillation amplitudes doubled. The piezo resonant frequency is quoted to be 315 kHz, which is approximately a factor of 100 larger than the frequency span used in our experiment. Being so far from resonance, it is reasonable to assume a flat frequency response of the piezo in our frequency range.

3. Spectra measurements

Spectra measurements are performed by a double-channel digital signal analyzer SR785 set in the swept-sine configuration. Spectra are acquired with 200 frequency points within the chosen frequency span. The analyzer

averages (as a digital lock-in) the input signal over 20 cycles of the frequency of each frequency point. The uncorrelated noise rejection is very high. The choice of 20 cycles was a compromise for a good noise rejection and a not-too-long spectra measuring time (a few seconds). Channel 1 of the double-channel digital signal analyzer is connected to the output of the interferometer 1 (Bubble 1) and channel 2 to the one of interferometer 2 (Bubble 2). With the swept-sine configuration, the two Bubble 1 and Bubble 2 spectra are acquired synchronously with the same sweeping sine wave voltage applied to the piezo transducer. It is also possible to acquire the cross spectrum of the two interferometer outputs. Due to the two-channel synchronization, the cross spectrum is able to give the relative phase of the two interferometric signals and hence of the oscillations of the two bubbles, as shown in Figure 3c of the main text.

The procedure used to measure the single-bubble response in the two-bubble experiment is the following. We form the first bubble and we measure its resonance frequency. Then we introduce the second bubble and perform the desired measurements of the two approaching bubbles. At the end we take the first bubble off and, being the second bubble left alone, we measure its resonance frequency.

4. Some design considerations

The interferometer of the present work is designed for minimum bubble radii of approximately 0,2 mm. The limitation is due to the focusing characteristic of the laser beam coming from the single-mode optical fiber. The laser spot size (transversal diameter of the beam) at the entrance of the bubble should be small with respect to the bubble diameter. We tailored the optics for a spot size of approximately 10 μm. With more complicate optics one can reduce the spot size and hence the minimum radius of the bubble. The laser has to have a sufficiently long coherence length (like, for instance, the one of a He-Ne laser). Many multimode diode lasers are not usable since their coherence length is too short to allow interference between the light reflected by the two interfaces of the bubble (see Figure 1 in the main text). For gas bubbles in water fringe visibility is excellent due to the large refractive index change between water and air. Photomultipliers (Hamamatsu type R2949 in our set-up) are known to be perfectly linear over several decades of incident light intensity. An interference filter in front of the photomultiplier blocks the background light at wavelengths different from the He-Ne one. Light is collected through a small hole (approximately one twentieth of the central fringe size). The light power at the bubble interface is approximately 3.5 mW, causing a perfectly visible fringe pattern in the backward direction (Figure 1S). Calibration of the interferometer is intrinsically given by the known laser wavelength (633 nm). With a photomultiplier gain of 10^4, a typical variation of 1 Volt on a load resistance of 50 kΩ is measured when the central fringe goes from maximum light to dark, that is, with $\Delta R = \lambda/8 = 79.1$ nm. A typical spectrum registered in the working frequency range from a bubble in absence of piezo excitation gives a noise value of the order of 0.3 mV, which means 0.023 nm of the noise background of radius measurement. This figure is even lower than the interferometer sensitivity of 0.1nm quoted in the main text (Raudino et al. 2017), this to take care of unpredictable environmental noise sources (such as an airplane flying over the lab!).

The interferometer response function (output given by the interferometer) has the form:

$$I(x) = A(I_1 + I_2 + 2(I_1 I_2)^{1/2} \cos(2\pi x/\lambda)),$$

where A is a constant which depends on the photodetection circuitry, I_1 and I_2 are the light intensities retro-reflected at the two bubble interfaces and x is their optical path difference (Corti et al. 2012). The interferometer can operate in a region where the response function I(x) is nearly linear with x, that is, around a point where $2\pi x/\lambda$ is equal to an odd multiple of $\pi/2$. In this case, a 1% deviation from linearity is reached with a vibration amplitude of 14 nm. The experiments reported in the present manuscript are all performed within this linear region. For larger vibration amplitudes the full response function should be used to connect the measured output with the vibration amplitude. Eventually fringe counting techniques can be used for very large amplitudes (mm and more). Of course, operation in the linear region is quite advantageous since it requires very simple circuitry.

5. Quasi-contact distances

Figure 4S reports an example of the sequence of spectra recorded as a function of the inter-bubble face-to-face distance (the spectra correspond to the bubbles mentioned in Figure 3(a,c) of the main text). The resonance peaks are well-resolved with clearly distinguishable amplitudes and are fitted by a Lorentz shape, as shown in Figure 5S. Amplitudes are normalized for the non-uniform pressure field described in Figure 3S.

The data reported in Figure 4S, as well as Figures 3(b,d), 4 and 5 of the main text, actually stop at a face-to-face distance of approximately 20 μm. Their behavior follows perfectly the predictions of the close-distance theoretical model when R1/h approaches R1/(R1+R2) and differs significantly from the long-distance model predictions (especially the high-frequency peaks). Closer distances pose some experimental difficulties concerning the precise determination of the distance, but are worth investigating. In Figure 6S we report an example of spectra for close bubble approach. As can be seen, the spectra lose their distinct two-peak (Lorentzian) feature.

6. Surface modes

As shown in Figure 1 of the main text, the interferometric technique can easily detect bubble surface modes, lying in the low-frequency range. Therefore, studies of bubble-bubble interactions via surface mode are quite possible. Nevertheless, in this case it is essential to be able to keep track of the surface properties, like surface tension, charge density and energy dissipation at the interface. A unique feature of our interferometric technique is that it makes these data readily available by a simple analysis of the frequency, amplitude and width of the mode resonance registered by the spectra. For the sign and amplitude of the interface charge an extra electrode should be introduced (simple to implement), in order to provide an electrical excitation of the bubble (Corti et al. 2012).
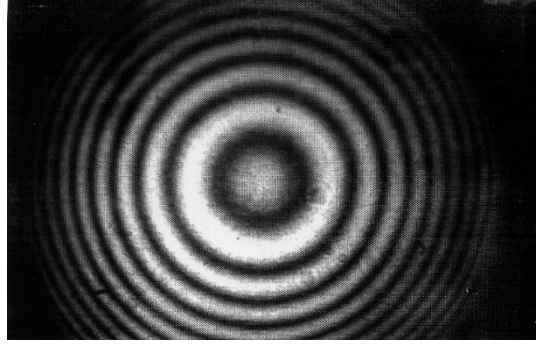
Figure 1S: Fringe pattern observed in the backward direction due to interference of the laser beam reflection at the two interfaces of the bubble (points S1 and S2 in Figure1 of the main text).
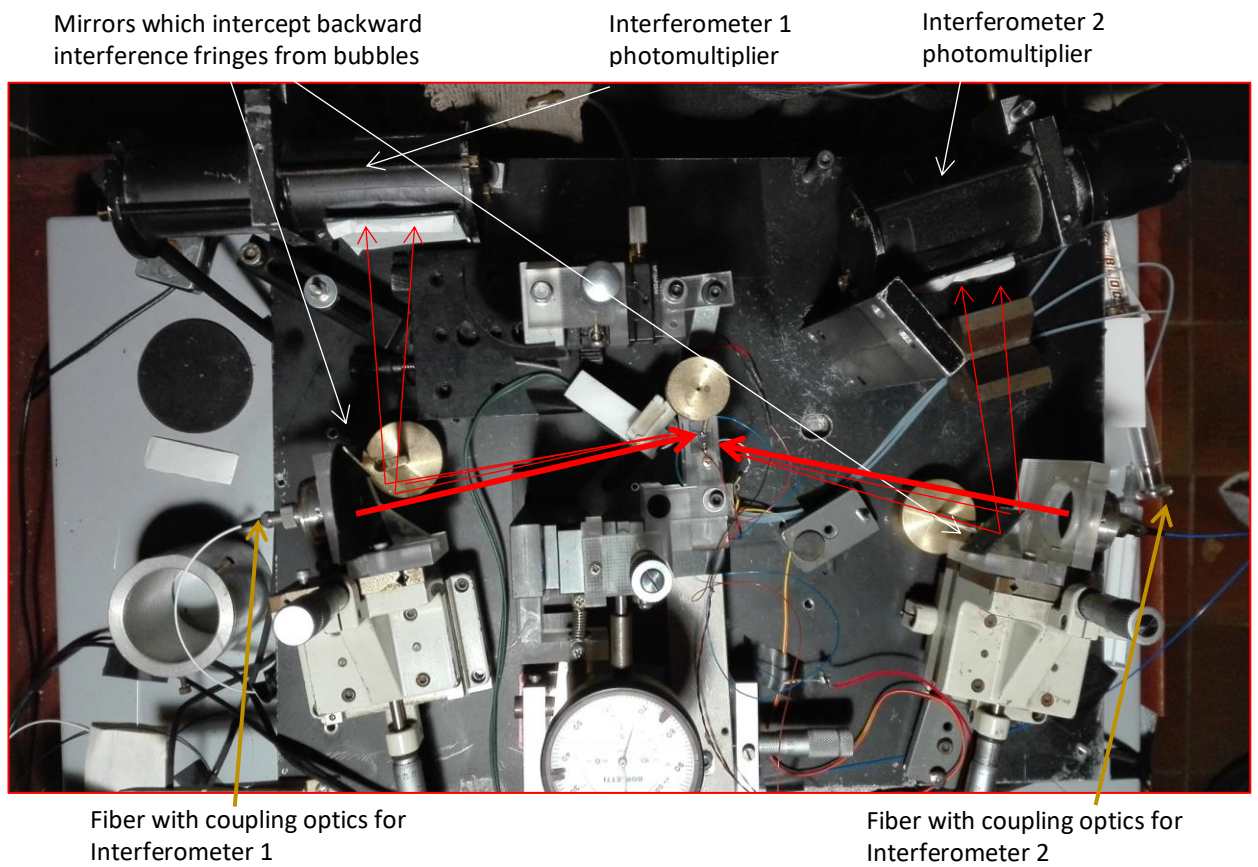

Mirrors which intercept backward interference fringes from bubbles

Interferometer 1 photomultiplier

Interferometer 2 photomultiplier

Fiber with coupling optics for Interferometer 1

Fiber with coupling optics for Interferometer 2

Figure 2S: Annotated picture (top view) of the double interferometer set-up used in our experiments (see also Figure 2 in the main text for a close-up of the measurement cell).
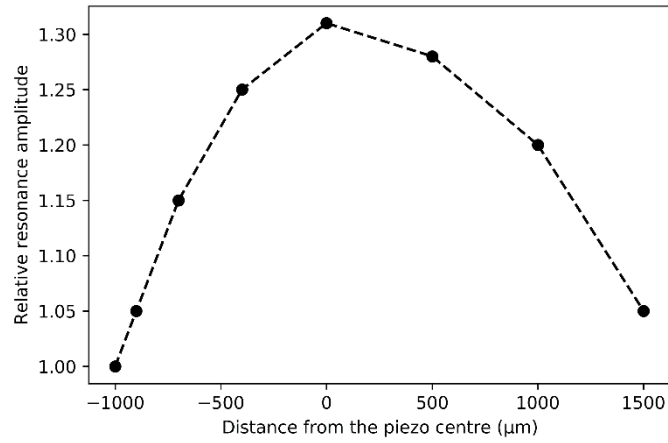
Figure 3S: Variation of (relative) resonance amplitudes along the horizontal line of bubble approach in the two-bubble experiments. The x=0 point corresponds to the center of the piezoceramic. These data were used to evaluate deviations from spatial uniformity of the pressure field. The peak amplitudes shown in the figures (e.g. Figure 4S) were normalized accordingly.
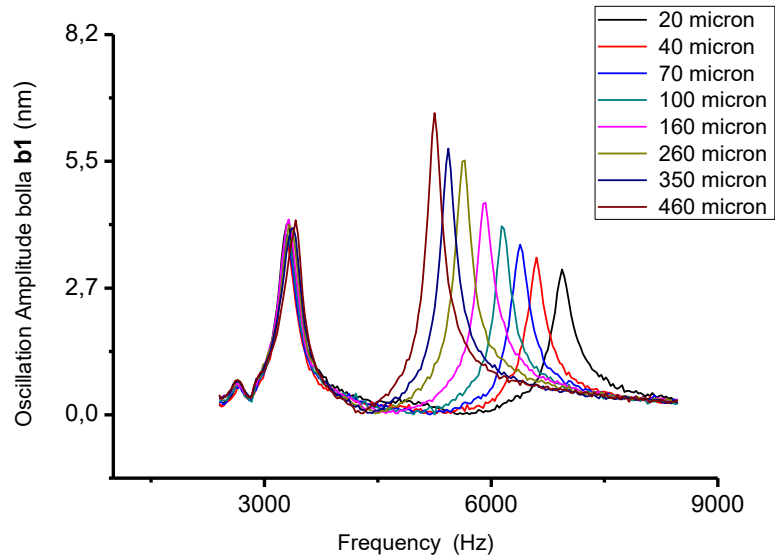

Figure 4S: Example of the sequence of spectra recorded as a function of the inter bubble face to face distance (spectra correspond to the Bubble 1 mentioned in Figure 3a of the main text).
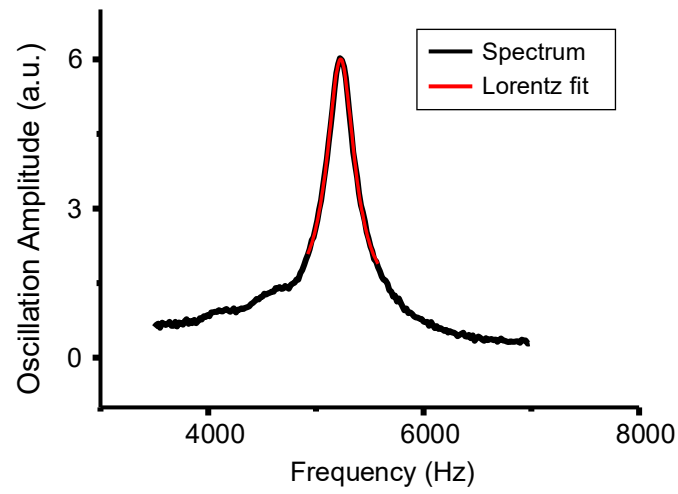
Figure 5S: Example of Lorentz fit (red line) quality of the measurement (black line) of a volume mode spectrum.
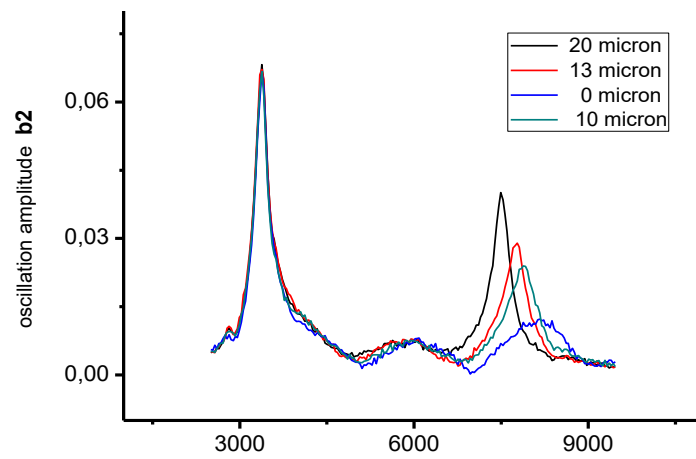

Figure 6S: Resonance frequencies in proximity of bubble-bubble contact. Here, x values are the excitation frequencies, in Hz; y values (expressed in arbitrary units) are proportional the oscillation amplitudes, of order of 1nm.